

Reversible Fluid Coupling Analysis

In this section we present a simple one-dimensional analysis of the flow in a reversible fluid coupling. This one-dimensional analysis may be used as a first order estimate of the coupling performance. Alternatively it can be applied to a series of stream tubes into which the coupling flow is divided. Such a multiple stream tube (or two-dimensional flow) analysis allows accommodation of the large variations in flow velocity and inclination that occur between the core and the shell of the machine.

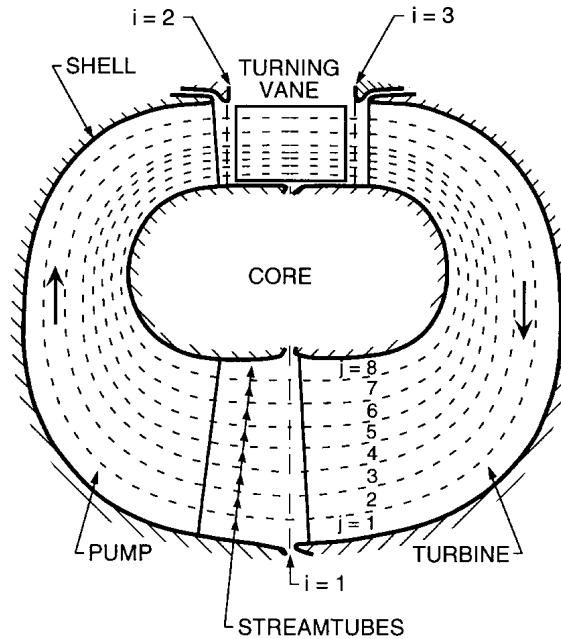


Figure 1: Sketch showing the subdivision of the flow into stream tubes.

In the multiple stream tube analysis the flow is subdivided into stream tubes as shown in Figure 1; all the data presented here used ten stream tubes of roughly similar cross-sectional area. The flow in each stream tube is characterized by meridional and tangential components of fluid velocity, u_i and v_i , at each of the transition stations, $i = 1, 2, 3$, between the turbine and the pump ($i = 1$), between the pump and the turning vanes ($i = 2$) and between the turning vanes and the turbine ($i = 3$). Note that the meridional component, $u_i = Q/A_i$, where Q is the volume flow rate of fluid and A_i is the cross-sectional area of flow at the location $i = 1, 2, 3$. A typical velocity triangle, in this case for the transition station $i = 1$, is included in Figure 2; the velocity triangles for the other transition stations are similar. Later we will present measured performance data for the reversible coupling whose basic geometry is listed in Table 1.

In the multiple stream tube analysis, the mean radius of the j th stream tube (divided by R) (the numbering of the stream tubes is shown in Figure 1) at each of the locations $i = 1, 2, 3$ is defined by $\bar{r}_{j,i}$. Since the distribution of velocity will change from one station to the other, only one of these three sets of stream tube radii can be selected *a priori*. We chose to select the series $\bar{r}_{j,1}$ at the turbine/pump transition. It follows that $\bar{r}_{j,2}$ and $\bar{r}_{j,3}$, the stream tube radii at the pump discharge and at the turning vane discharge must then be calculated as a part of the solution. Discussion of how this is accomplished is postponed until the solution methodology is described.

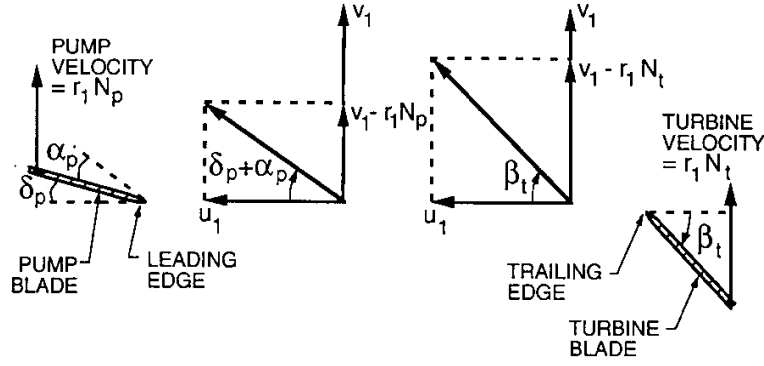


Figure 2: Velocity triangle at the turbine/pump transition station, $i = 1$. Flow is from the right to left, the direction of rotation is upward and the angles are shown as they are when they are positive.

Table 1: Basic geometric data for the particular reversible coupling analyzed here. Angles are relative to the axial plane. Outer shell radius, R , is $0.5m$.

Pump discharge vane angle, β_p , at shell	0°
Pump discharge vane angle, β_p , at core	0°
Turbine discharge vane angle, β_t , at shell	31.5°
Turbine discharge vane angle, β_t , at core	44°
Turning vane discharge angle, β_v	-55°
Pump inlet vane angle, δ_p , at shell	-17°
Pump inlet vane angle, δ_p , at core	-10°
Turbine inlet vane angle, δ_t , at shell	0°
Turbine inlet vane angle, δ_t , at core	0°
Turning vane inlet angle, δ_v	55°
Outer core radius/Outer shell radius, r_b	0.861
Inner core radius/Outer shell radius, r_c	0.592
Inner shell radius/Outer shell radius, r_d	0.29

The process of power transmission through the coupling (operating under steady state conditions) will now be delineated. In the process, several loss mechanisms will be identified and quantified so that a realistic model for the actual interactions between the mechanical and fluid-mechanical aspects of coupling can be achieved.

Pump

The power input to the pump shaft is clearly $\Omega_p T_p$ where Ω_p is the angular velocity of the pump (rad/s) and T_p is the shaft torque for the pump. Some of the power is consumed by windage losses in the fluid annulus between the pump shell and the stationary housing. This is denoted by a pump windage torque, T_{pw} , which will be proportional to Ω_p^2 . Included in this loss will be the shaft seal loss as it has the same functional dependence on pump speed. It is convenient to denote this combined windage and seal torque, T_{pw} , by a dimensionless coefficient, C_{pw} , where $T_{pw} = C_{pw} \rho R^5 \Omega_p^2$ and ρ denotes the fluid density. Appropriate values of C_{pw} can be obtained, for example, from Balje (1981) who suggests values of the order of 0.005.

Furthermore the labyrinth seal in the core between the pump and turbine rotors causes direct transmission of torque from the pump shaft to the turbine shaft. This torque which is proportional to $(\Omega_p - \Omega_t)^2$ will

be denoted by T_s and is represented by a seal windage torque coefficient, C_{sw} , defined as

$$T_s = C_{sw}\rho R^3(r_b^2 - r_c^2)(\Omega_p - \Omega_t)^2 \quad (\text{Mec1})$$

A comparison with the experimental data (see below) suggests a value of C_{sw} of about 0.014. Regarding this labyrinth seal, we should also observe that the leakage through this seal has been neglected in the present analysis.

It follows that the power available for transmission to the main flow through the pump is $\Omega_p(T_p - T_{pw} - T_s)$ and this manifests itself as an increase in the total pressure of the flow as it passes through the pump. For simplicity, the present discussion will employ a two-dimensional representation of the fluid flow in which the flow is characterized at any point in the circuit by a single meridional velocity, u_i , and a single tangential velocity, v_i , at the appropriate rms radius. In practice, these quantities will vary over the cross section of the flow and this variation is considered later. At this stage it is not necessary to introduce this complexity. The power balance between the mechanical input, the losses and the ideal fluid power applied to the pump, then yields

$$\Omega_p(T_p - T_w - T_s) = QH_{pi} \quad (\text{Mec2})$$

where, from the application of angular momentum considerations in the steady flow between pump inlet ($i = 1$) and pump outlet ($i = 2$), the ideal pump head rise, H_{pi} , is given by

$$H_{pi} = \rho\Omega_p(r_2v_2 - r_1v_1) \quad (\text{Mec3})$$

where r_1 , r_2 are the radial locations (in m) of the inlet and outlet and v_1 , v_2 are the tangential components of velocity at those locations. More specifically, H_{pi} is ideal pump total pressure rise in the absence of fluid viscosity when the pump would be 100% efficient. However, in a real, viscous flow, the actual total pressure rise produced, H_p , is less than H_{pi} ; the deficit is denoted by H_{pl} where

$$H_p = H_{pi} - H_{pl} \quad (\text{Mec4})$$

This total pressure loss, H_{pl} , is difficult to evaluate accurately and is a function, among other things, of the angle of attack on the leading edges of the vanes. Note that the angle of attack (relative to the axial plane), α_p , on the pump blades is given by

$$\alpha_p = \tan^{-1} \left\{ \frac{v_1 - r_1\Omega_p}{u_1} \right\} - \delta_p \quad (\text{Mec5})$$

In the present context the total pressure loss, H_{pl} , is ascribed to two coefficients, C_{pa} , and C_{pb} . The first coefficient, C_{pa} , describes a loss which is a fraction of the dynamic pressure based on the component of relative velocity parallel to the blades at the pump inlet. The second coefficient, C_{pb} , describes a loss that is a fraction of the dynamic pressure based on the component of the pump inlet relative velocity perpendicular to the blades. Thus

$$H_{pl} = \frac{\rho}{2} [u_1^2 + (v_1 - r_1\Omega_p)^2] [C_{pa} + (C_{pb} - C_{pa})\sin^2\alpha_p] \quad (\text{Mec6})$$

The coefficients C_{pa} and C_{pb} can be estimated using previous experience in pumps. Though there are many possible representations of the pump total pressure loss, the above form has several advantages. First, at a given flow rate, the loss is appropriately a minimum when α_p is zero, a condition which would correspond to the design point in a conventional pump. And this minimum loss is a function only of C_{pa} . On the other hand at shut-off (zero flow rate) the loss is a function only of C_{pb} . These relations permit fairly ready evaluation of C_{pa} and C_{pb} in conventional pumps given the head rise and efficiency as a function of flow

rate. Typical values of C_{pa} and C_{pb} are of the order of unity; but the value of C_{pa} must be less than the value of C_{pb} , the difference representing the effect of the inlet vane angle on the losses in the pump.

The hydraulic efficiency of the pump, η_p , is $1 - H_{pl}/H_{pi}$. In a conventional centrifugal pump for which $v_1 = 0$, the maximum design point efficiency, η_p , is expected to be about 0.85. With the kind of uneven inlet flow to be expected in the present flow a lower value of the order of 0.80 is more realistic. This value provides one relation for C_{pa} and C_{pb} .

Turbine

We now jump to the turbine output shaft and work back from there. The power delivered to the turbine shaft is $\Omega_t T_t$ where Ω_t is the angular velocity of the turbine (*rad/s*) and T_t is the shaft torque for the turbine. As in the pump there are windage losses, $\Omega_t T_{tw}$, where the windage torque, T_{tw} , is described by a dimensionless coefficient, $C_{tw} = T_{tw}/\rho\Omega_t^2$. Then the power delivered to the turbine rotor, $\Omega_t(T_t + T_{tw} - T_s)$, by the main flow through the turbine is related to the ideal total pressure drop through the turbine, H_{ti} , by

$$\Omega_t(T_t + T_{tw} - T_s) = QH_{ti} \quad (\text{Mec7})$$

where, again, from angular momentum considerations

$$H_{ti} = \Omega_t(r_2 v_3 - r_1 v_1) \quad (\text{Mec8})$$

With an inviscid fluid, H_{ti} would be the actual total pressure drop across the turbine. But in a real turbine the actual total pressure drop is greater by an amount, H_{tl} , which represents the total pressure loss in the turbine, and hence

$$H_t = H_{ti} + H_{tl} \quad (\text{Mec9})$$

In a manner analogous to that in the pump, the total pressure loss in the turbine, H_{tl} , is ascribed to two coefficients C_{ta} and C_{tb} . The first coefficient, C_{ta} , describes a loss which is a fraction of the dynamic pressure based on the component of relative velocity parallel to the blades at the turbine inlet. This coefficient essentially determines the minimum loss at the design point where the angle of attack, α_t , is zero. The second coefficient, C_{tb} , describes a loss which is a fraction of the dynamic pressure based on the component of the turbine inlet velocity perpendicular to the blades. Thus

$$H_{tl} = \frac{\rho}{2} [u_3^2 + (v_3 - r_3\Omega_t)^2] [C_{ta} + (C_{tb} - C_{ta})\sin^2\alpha_t] \quad (\text{Mec10})$$

where the the angle of attack (relative to the axial plane), α_t , on the turbine blades is given by

$$\alpha_t = \tan^{-1} \left\{ \frac{v_3 - r_2\Omega_t}{u_3} \right\} - \delta_t \quad (\text{Mec11})$$

As in the case of the pump, appropriate values of C_{ta} and C_{tb} are of the order of unity and should be such as to yield a stand-alone turbine efficiency, H_{ti}/H_t of the order of 0.85. However, C_{tb} must be greater than C_{ta} to reflect the appropriate effect of the inlet vane angles on the hydraulic losses.

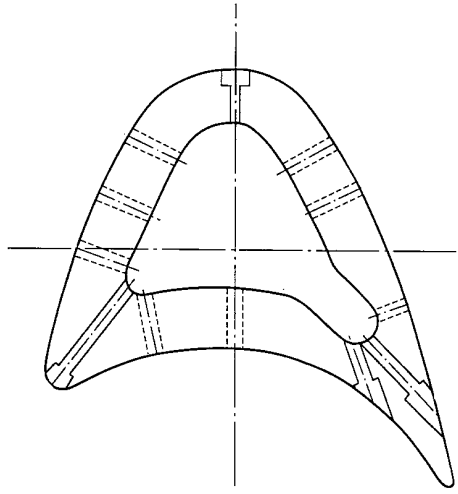


Figure 3: Cross-section of a turning vane.

Turning Vanes

The geometry of a turning vane used in the coupling discussed here is shown in Figure 3.

The total pressure rise produced by the pump, H_p , is equal to the total pressure drop across the turbine, H_t , plus the total pressure drop across the turning vanes, H_v , so that

$$H_p = H_t + H_v \quad \text{with the turning vanes inserted} \quad (\text{Mec12})$$

$$H_v = 0 \quad \text{with the turning vanes retracted} \quad (\text{Mec13})$$

It is this balance which essentially determines the flow rate, Q , and the meridional velocities, u_i . The total pressure drop across the vanes, H_v , is described a loss coefficient defined by

$$C_v = 2H_v / \rho(v_3^2 + u_3^2) \quad (\text{Mec14})$$

Though both H_v and C_v will vary with the angle of attack of the flow on the turning vanes, α_v , we have not exercised that option here since there is no independent information on the turning vane performance. Estimates from experience suggest that C_v should lie somewhere between about 0.3 and 1.0.

Turbine Partial Admission Effect

Due to the large blockage effects of the turning vanes, the flow discharging from the vanes consists of an array of jets interspersed with relatively stagnant vane wakes. This means that during reverse operation the turbine experiences inlet conditions similar to those in a partial admission turbine. In the hydraulic analysis we can approximately account for these partial admission effects by taking note of the following property of partial admission. Consider and compare the flux of angular momentum in the flow into the turbine, first, for full admission and, second, for partial admission. Under uniform, full admission conditions, u_3 and v_3 are independent of circumferential position and the flux of angular momentum entering the turbine is proportional to $u_3 v_3$. If the swirl angle were defined by the turning vane discharge angle then this reduces to $u_3^2 \tan \beta_v$. On the other hand a partial admission flow consisting of jets with velocity components u_3^* , v_3^*

alternating with stagnant wakes of zero velocity would have a flux of angular momentum equal to $ku_3^*v_3^*$ where k is the fraction of the cross-sectional area occupied by the jets ($0 < k < 1$). But if the total flow rate is the same in both cases then $u_3^* = u_3/k$ and if the jets are parallel with the turning vane discharge angle then $v_3^* = u_3^* \tan \beta_v$. Hence the flux of angular momentum becomes $u_3^2 \tan \beta_v/k$. In other words the blockage which creates the jets and wakes also leads to an *increase* in the flux of angular momentum by the factor, $1/k$.

To account for this in the flow analysis, the appropriate angular momentum flux (which is essential to the basic principles of the pump or turbine) can be maintained by inputting an *effective* turning vane discharge angle denoted by β_v^* . Comparing the above expressions the effective turning vane discharge angle is given by

$$\tan \beta_v^* = \tan \beta_v/k \quad (\text{Mec15})$$

Hence by inputting a somewhat larger than actual turning vane discharge angle we can account for these partial admission effects.

The problem therefore reduces to estimating an appropriate value for k from the experimental measurements. For this purpose, we develop the relation between k and the loss coefficient for the turning vanes, C_v . If the total head of the jets is assumed to be equal to the upstream total head (at location $i = 2$), then it is readily shown that the *mean* total head of the discharge (including the wakes) implies the following relation between k and C_v :

$$k = \left\{ \frac{1 - C_v \tan^2 \beta_v}{1 + C_v} \right\}^{\frac{1}{2}} \quad (\text{Mec16})$$

The value of $C_v = 0.36$ which is deployed later along with the appropriate $\beta_v = -55^\circ$ yield $\beta_v^* = -72.8^\circ$ and a blockage ratio (or partial emission factor) of $k = 0.44$ which seems reasonable given the geometry of the turning vane cascade.

Solution for an individual stream tube:

Consider first the solution of the flow in an individual stream tube where it is assumed that the velocity at any location in the circular path (Figure 1) can be characterized by a single meridional and a single tangential velocity. Assume for the moment that the radial positions of the stream tube are known; then the inlet and discharge angles encountered by that particular stream tube at those radial positions at each of the transition stations can be determined. Then, for a given slip, $S = 1 - \Omega_t/\Omega_p$, the first step is to solve the flow equation (Mec12) or more specifically:

$$H_{pi} - H_{pl} = H_{ti} + H_{tl} + H_v \quad (\text{Mec17})$$

to obtain the flow rate and velocities. The procedure used starts with a trial value of u_1 . Values of u_2, u_3 follow from continuity knowing the areas A_i :

$$u_i = u_1 A_1 / A_i \quad , \quad i = 2, 3 \quad (\text{Mec18})$$

Furthermore, it is assumed that the relative velocity of the flow discharging from the pump, the turning vanes or the turbine is parallel with the blades of the respective device (or the effective angle in the case of the turning vanes). Given the high solidity of the pump and turbine, this is an accurate assumption. This allows evaluation of the tangential velocities:

$$v_1 = r_1 \Omega_t + u_1 \tan \beta_t \quad (\text{Mec19})$$

$$v_2 = r_2 \Omega_p + u_2 \tan \beta_p \quad (\text{Mec20})$$

where r_1 and r_2 are rms channel radii at each location and $v_3 = v_2$ for the turning vanes retracted and $v_3 = u_3 \tan \beta_v$ for the turning vanes inserted. These relations can then be substituted into the definitions (Mec3), (Mec8), (Mec6), (Mec10) and (Mec14) to allow evaluation of all the terms in equation (Mec17). That equation is not necessarily satisfied by the initial trial value for u_1 . Hence an iteration loop is executed to find that value of u_1 which does satisfy equation (Mec17). The velocities and flow rate are thus determined for a given value of the slip.

Multiple stream tube Solution:

As described in the last section, the multiple stream tube analysis begins with a set of guessed values for the stream tube locations at the transition stations, $i = 2$ and $i = 3$. It also begins with an assumed value for the flow rate in each stream tube (more specifically an assumed value of $u_1 = 1$.) Then the method of the last section is used to solve for the flow and allows evaluation of the total pressure changes and losses in each stream tube. Then, the degree to which equation (Mec17) is satisfied is assessed. This leads to an improved value of u_1 and the process is repeated to convergence (only three or four cycles are necessary). By doing this for each stream tube we obtain the total pressure and the static pressure differences between all three locations for each stream tube.

The principle by which the stream tube geometry is adjusted is that the flows in each of the three locations should be in radial equilibrium. This implies that, at each of the locations $i = 1, 2, 3$, the flow must satisfy

$$\left(\frac{\partial P}{\partial r} \right)_i = \frac{\rho v_i^2}{r_i} \quad (\text{Mec21})$$

where P is the static pressure. Application of this condition at the turbine/pump transition station ($i = 1$) establishes the static pressure difference between each stream tube. Then using the information from the flow solution on the static pressure differences between transition stations we can establish the pressure distribution between the stream tubes at transition stations $i = 2$ and $i = 3$. Then using equation (Mec21) we examine whether the flows in these locations are in radial equilibrium. Given the initial trial values of $\bar{r}_{j,2}$ and $\bar{r}_{j,3}$, this will not, in general, be true. The method adjusts the values of $\bar{r}_{j,2}$ and $\bar{r}_{j,3}$ and then repeats the entire process until radial equilibrium is indeed achieved at transition stations $i = 2$ and $i = 3$. This requires as many as 30 iterations.

Power Transmission Summary:

This completes the description of the power transmission through the coupling which is summarized in Table 2. The overall efficiency of the coupling, η , is given by

$$\eta = \frac{\Omega_t T_t}{\Omega_p T_p} = \frac{Q H_{ti} - \Omega_t T_{tw} + \Omega_p T_s}{Q H_{pi} + \Omega_p T_{pw} + \Omega_p T_s} \quad (\text{Mec22})$$

or substituting from equations (Mec4) and (Mec9):

$$\eta = \frac{\Omega_t (r_2 v_3 - r_1 v_1) - (\Omega_t T_{tw} + \Omega_t T_s) / Q}{\Omega_p (r_2 v_2 - r_1 v_1) + (\Omega_p T_{pw} + \Omega_p T_s) / Q} \quad (\text{Mec23})$$

Table 2: Power transmission and losses.

Pump shaft power	$= \Omega_p T_p$
Power lost in pump windage	$= \Omega_p T_{pw}$
Power to turbine through seal	$= \Omega_p T_s$
Power to main pump flow	$= QH_{pi}$
	$= \Omega_p (T_p - T_{pw} - T_s)$
Power in main flow out of pump	$= Q(H_{pi} - H_{pl})$
Power lost in turning vanes	$= QH_v$
Power in flow entering turbine	$= Q(H_{pi} - H_{pl} - H_v)$
	$= Q(H_{ti} + H_{tl})$
Power to turbine rotor by flow	$= QH_{ti}$
	$= \Omega_t (T_t + T_{tw} - T_s)$
Power to turbine through seal	$= \Omega_t T_s$
Power lost in turbine windage	$= \Omega_t T_{tw}$
Turbine shaft power	$= \Omega_t T_t$

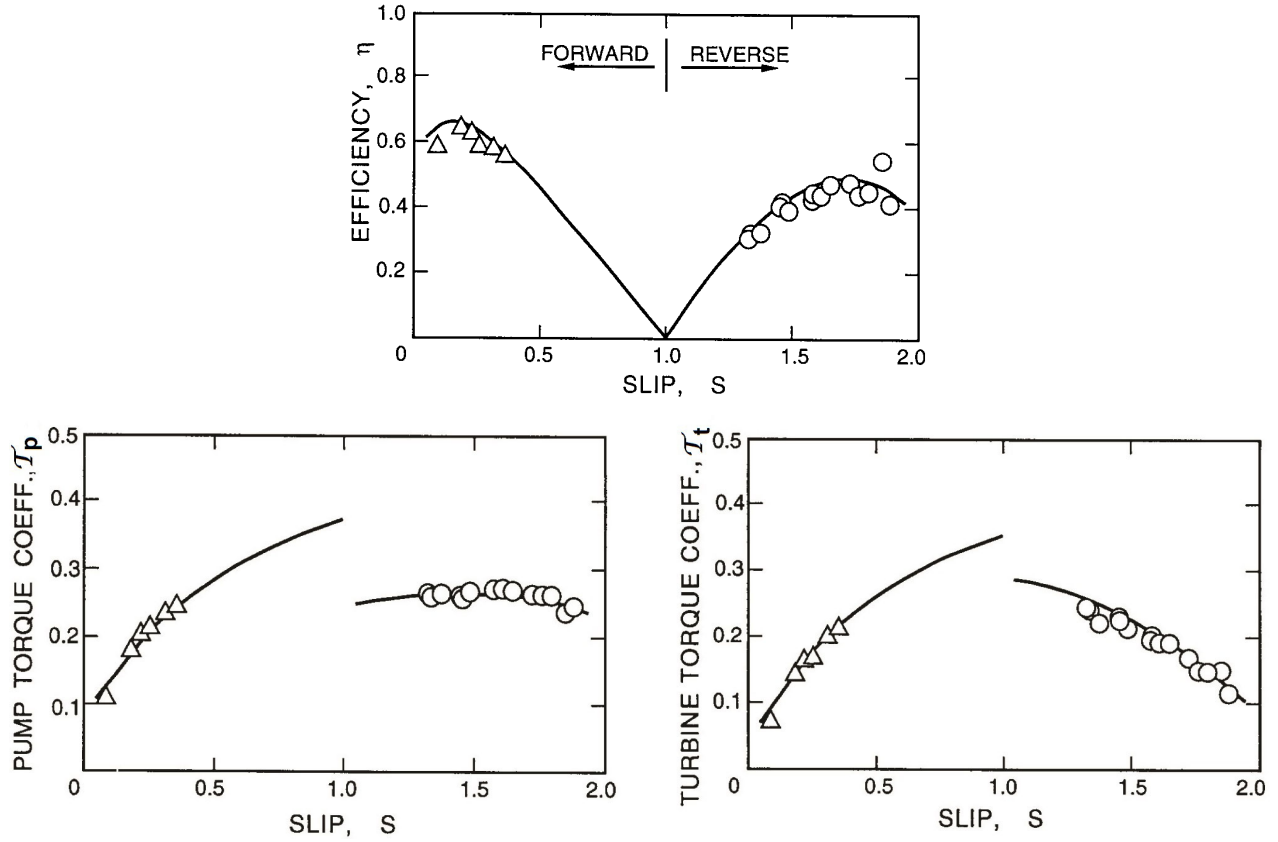


Figure 4: Efficiency and torque coefficients for the reversible coupling using $C_{pa} = C_{ta} = 0.7$, $C_{pb} = C_{tb} = 1.0$, $C_v = 0.36$, $C_{sw} = 0.02$, $C_w = 0.005$ and an effective turning vane discharge angle of -72.8° .

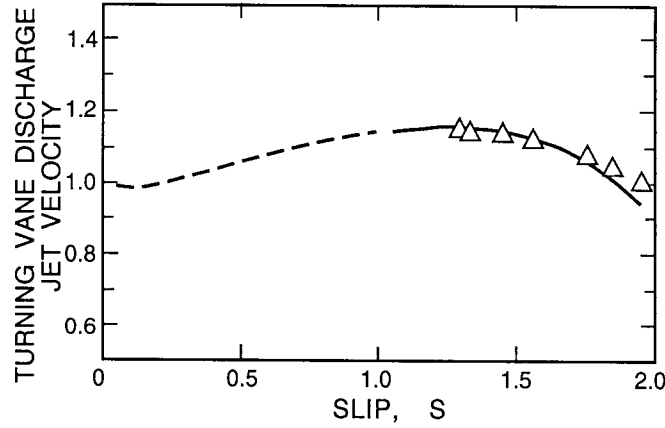


Figure 5: Velocity of turning vane discharge jets for the same conditions as listed in Figure 4.

This expression demonstrates an important feature of the reversible coupling. In the forward mode with the vanes removed, $v_2 = v_3$, and the quantities in parentheses in the numerator and denominator are identical. Therefore, if the windage torques, T_{tw} and T_{pw} , are small (as is normally the case) and if Q is not close to zero (as can only happen close to $S = 0$) then the coupling efficiency is close to $\Omega_t/\Omega_p = 1 - S$ (S is the slip). Thus, in the forward mode, only the windage losses cause the efficiency to deviate from $1 - S$. On the other hand no such simple relation exists in the reverse mode.

Apart from the overall efficiency, η , two other coupling characteristics will be presented, namely the pump torque coefficient, \mathcal{T}_p , and the turbine torque coefficient, \mathcal{T}_t . The pump torque coefficient is defined as $\mathcal{T}_p = T_p/\rho R^5 \Omega_p^2$ and the turbine torque coefficient by $\mathcal{T}_t = T_t/\rho R^5 \Omega_p^2$. Note the choice of Ω_p in the denominator for \mathcal{T}_t .

Comparison with experimental data:

The efficiency, torque coefficients and fluid velocities measured during tests of the coupling conducted by NAVSSES (using an oil of density 849 kg/m^3) at a input (or pump) speed of 1000 rpm will be compared to the results of the present analytical model. Note that although three graphs for η , \mathcal{T}_p and \mathcal{T}_t are presented, these only represent two independent sets of data since $\eta = \mathcal{T}_t(1 - S)/\mathcal{T}_p$.

A typical set of results for the performance of the coupling are presented in Figures 4 and 5. The coefficients C_{pa} , C_{pb} , C_{ta} , C_{tb} , and C_{va} (and, to a lesser extent, C_w and C_{sw}) were chosen to match the experimental data by proceeding as follows. First note that C_w and C_{sw} have little effect *except* close to $S = 0$. In fact, the peak in η near $S = 0$ is almost entirely determined by C_w and values of $C_w = 0.02$ were found to fit the data near $S = 0$ quite well. This value is also consistent with previous experience on windage coefficients (Balje 1981). Similarly past experience would suggest a value of 0.005 for the seal windage coefficient, C_{sw} .

Turning to the pump, turbine and turning vane loss coefficients, it is clear that the turning vanes have no effect on forward performance ($S < 1$). Hence the pump and turbine loss coefficients were chosen to match this data. In this regard the efficiency is of little value since the forward efficiency is always close to $(1 - S)$. Values of $C_{pa} = C_{ta} = 0.7$ and $C_{pb} = C_{tb} = 1.0$ seemed to match the forward torque coefficients well. These could be supported by the argument that all the dynamic head normal to the vanes at inlet will likely be lost (thus $C_{pb} = C_{tb} = 1.0$) and a high fraction of that parallel with the vanes is also likely

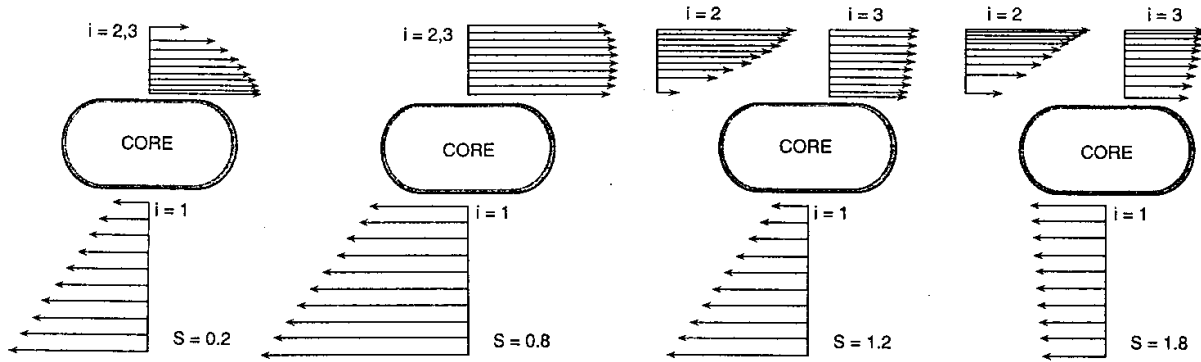


Figure 6: Meridional velocity distributions at the transition stations for four different slip values.

to be lost (thus $C_{pa} = C_{ta} = 0.7$). Note that the results presented are not very sensitive to the precise values used for these loss coefficients. It should also be noted that these loss coefficients yield sensible peak efficiencies for the pump or turbine when these are evaluated for stand-alone performance (respectively 79% and 86%).

Finally, then, we turn to the reverse performance ($S > 1$) with only one loss coefficient left to determine, namely the loss due to the turning vanes, C_{va} . In the example shown a value of C_{va} of 0.36 yields values of the efficiency that are consistent with the experimental results.

Note that if the coefficients described above were used with the actual turning vane discharge angle, there would be substantial discrepancies between the observed and calculated results; this helps to validate the present analysis and the use of the effective turning vane discharge angle, $\beta_v^* = -72.8^\circ$.

The multiple stream tube approach also provides information on the distributions of flow, angles of attack, etc. within the coupling and demonstrates how these change with slip. Examination of the results revealed several ubiquitous non-uniformities and one example, presented in Figure 6, will suffice to illustrate these. At low slip values in forward operation the meridional velocity profiles are very non-uniform. This non-uniformity consists of much higher meridional velocities near the axis in the turbine-to-pump transition and at the outer radius in all the transitions. As the slip increases in forward operation this non-uniformity decreases; near $S = 1$ it has disappeared at the pump-to-turbine transition but remains at the turbine-to-pump transition. When the turning vanes are inserted, the velocity profiles show a highly non-uniform character in the pump-to-turning-vane transition but this is almost completely evened out by the turning vanes. The turbine-to-pump non-uniformity near $S = 1$ is not too dissimilar to that in forward operation near $S = 1$. However, it is interesting to note that this non-uniformity is reversed as $S = 2$ is approached. These changing non-uniformities are important because they imply corresponding changes in the distribution of the angles of attack on the pump, turning vanes, and turbine. Consequently, the optimal vane inclination distributions (which would have as their objective uniform angles of attack) are different for forward and reverse operation.

In conclusion, we have presented a hydraulic analysis of a reversible fluid coupling operating over a range of slip values in both forward ($0 < S < 1$) and reverse ($1 < S < 2$) operation. The analysis employs estimated loss coefficients for the pump, turbine, turning vanes, windage and core seal. It splits the flow into an array of stream tubes with pressure balancing adjustment across those stream tubes and solves to find the fluid velocities, flow rates and static pressures at each of the transition stations for each stream tube. This information then allows evaluation of the overall performance characteristics including the efficiency and the pump and turbine torque coefficients. Comparison with data from the full scale testing (conducted by

the US Navy) of a reversible fluid coupling made by Franco-Tosi demonstrates good agreement between the analysis and the experiments. While the analysis involves the selection and identification of a number of hydraulic loss coefficients, the values of the coefficients do appear to be valid over a wide range of operating points, slip values and speeds. Moreover, though these coefficients are necessarily specific to the particular coupling studied, they nevertheless provide benchmark guidance for this general class of machine.

When the coupling is operated in the forward mode, the flow rates are small and hence the hydraulic losses are quite minor. Thus the efficiency is close to the ideal. However, as the slip increases, the flow rates become larger and the hydraulic losses (which increase like the square of the flowrate) become substantial. Under these conditions the device behaves much more like an interconnected pump and turbine than a conventional fluid coupling and the overall efficiency is similar to that one would expect from a device which links drive trains through a combination of a pump and a turbine. Even under the best of circumstances the analysis suggests that the efficiency of this generic type of coupling could not be expected to exceed 60% in the reverse mode.

The analysis presented here also demonstrates that, since it is used over a wide range of slip values, a reversible fluid coupling must operate over a wide range of angles of attack of the flows entering the pump and turbine rotors. With fixed geometry rotors, this inevitably results in substantial hydraulic losses, particularly in the reverse mode. Choosing the inlet blade angles in order to minimize those losses is not simple and it is not clear how the fixed geometry should be chosen in order to achieve that end.